JACS
JOURNAL OF THE AMERICAN CHEMICAL SOCIETY

Communication

pubs.acs.org/JACS

Model System for Cell Adhesion Mediated by Weak Carbohydrate–Carbohydrate Interactions

Bärbel Lorenz,[†] Luis Álvarez de Cienfuegos,[¶] Marieelen Oelkers,[†] Ella Kriemen,[‡] Christian Brand,[‡] Milena Stephan,[†] Eva Sunnick,[†] Deniz Yüksel,[§] Venkateshwarlu Kalsani,[§] Krishna Kumar,[§] Daniel B. Werz,[‡] and Andreas Janshoff*[,†]

[†]Institute of Physical Chemistry and [‡]Institute of Organic and Biomolecular Chemistry, University of Göttingen, Tammannstrasse 6, 37077 Göttingen, Germany

[§]Department of Chemistry, Tufts University, 62 Talbot Avenue, Medford, Massachusetts 02155, United States

[¶]Department of Organic Chemistry, Universidad de Granada, Granada, Spain

Supporting Information

ABSTRACT: The multivalent carbohydrate–carbohydrate interaction between membrane-anchored epitopes derived from the marine sponge *Microciona prolifera* has been explored by colloidal probe microscopy. An *in situ* coupling of sulfated and non-sulfated disaccharides to membrane-coated surfaces was employed to mimic native cell–cell contacts. The dynamic strength of the homomeric self-association was measured as a function of calcium ions and loading rate. A deterministic model was used to estimate the basic energy landscape and number of participating bonds in the contact zone.

Weak interactions between glycoconjugates displayed on cell surfaces play a pivotal role in cell adhesion, and further in cell development, fertilization, metastasis, myelin compaction, and cell aggregation in sponges.[1] In marine sponges, dissociated cells can reaggregate through calcium-mediated association of cell-surface proteoglycans (aggregation factors) in a species-specific manner.[2−4] There is growing evidence that carbohydrate recognition in marine sponges such as *Microciona prolifera* could be the allogeneic determinant of sponge self-/non-self-recognition. This may have provided the basis for early metazoans ability to resist the negative effects of chimerism, for instance, the insertion of fitness-reducing genes.[5] For cell–cell adhesion two polyvalent domains of the proteoglycan *M. prolifera* aggregation factor (MAF) are important. MAF is composed of two *N*-glycosylated proteins, MAFp3 and MAFp4; the former carries copies of a 200 kDa acidic glycan (g-200), whereas the latter possesses about 50 copies of a 6 kDa glycan (g-6).[1] The MAFp4 arms of the sunburst-like proteoglycans are linked cell-surface binding receptors, while the exposed g-200 glycans of the MAFp3 ring participate in calcium-dependent self-association. Two oligosaccharide epitopes, the pyruvated trisaccharide β-D-Gal(4,6-(*R*)-Pyr)-(1→4)-β-D-GlcNAc(1→3)-α-L-Fuc and the sulfated disaccharide β-D-GlcNAc(3S)-(1→3)-α-L-Fuc, have been shown to be essential for cell–cell interactions in *M. prolifera*.[6,7]

The measurement of forces governing self-association of biologically significant carbohydrates at the single molecule level with minimal influence from non-specific interactions in a native-like environment poses a significant experimental challenge. Recently, Anselmetti and co-workers were able to measure the self-recognition of g-200 as a function of Ca^{2+} in solution using single-molecule force spectroscopy.[5] Synthetic derivatives of the sulfated disaccharide coupled to bovine serum albumin,[8] gold nanoparticles,[9,10] and gold-coated AFM tips,[11] unambiguously showed that the presence of Ca^{2+} is necessary to induce the required conformational changes to stabilize dimers formed by the sulfated disaccharide β-D-GlcNAc(3S)-(1→3)-α-L-Fuc.[11]

One of the major experimental problems in studying multivalent binding of otherwise weak cell surface based non-covalent bonds is the interference by non-specific forces due to the absence of the natural matrix, the plasma membrane.[4] The fluidity of the bilayer paired with an abundance of choline headgroups disfavors non-specific interactions to a large extent. Moreover, Helfrich repulsion due to thermal undulation and steric repulsion of the glycocalyx prevents biomembranes from adhering easily.[12] Apart from these technical issues, the impact of lateral organization on affinity and vice versa is of great interest in binding cooperativity.[13]

Here, we present a versatile platform based on colloidal probe microscopy employing lipid bilayer-coated surfaces that allows measurement of weak multivalent carbohydrate–carbohydrate interactions in a native-like environment. Scheme 1a shows the chemical structure of the two disaccharide epitopes derived from *M. prolifera* used in this study (see SI for their synthesis). The disaccharides **1** and **2** were covalently coupled to preformed lipid bilayers through conjugation of the free thiol group to a maleimide moiety on a fraction of phospholipids to control the number of carbohydrate groups displayed.[14−16] Since thermal undulation of lipid bilayers renders analysis of binding affinity cumbersome, we used solid-supported membranes (SSMs) which preserve fluidity but suppress spatial bilayer fluctuations. Fluidity is crucial considering that lateral organization of ligand-receptors into clusters as a result of competition between binding enthalpy and mixing entropy is only possible in laterally mobile matrices.[17,18]

The general setup of our experiment involves a membrane-coated borosilicate sphere with a diameter of 15 μm attached

Received: November 2, 2011
Published: January 31, 2012

Scheme 1. Experimental Setup[a]

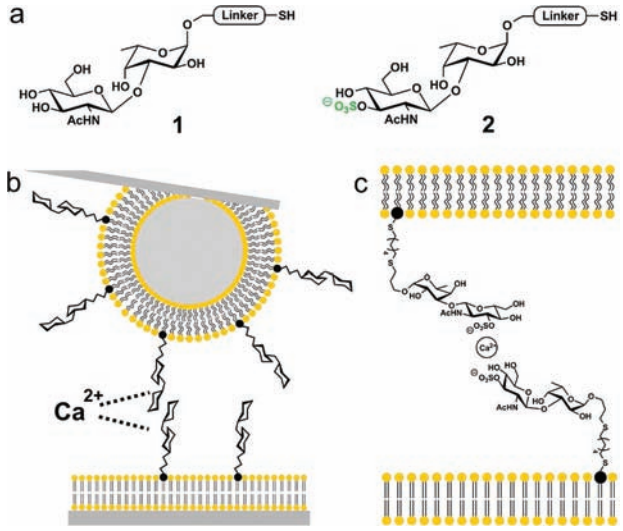

[a]Structure of disaccharides **1** and **2** (a) probed by colloidal force microscopy employing membrane-coated surfaces (b). The disaccharides are covalently coupled to the lipid bilayer through maleimide chemistry allowing the probing of interaction forces as a function of calcium ion concentration (c).

to a tip-less cantilever (Scheme 1b). The silicate sphere is coated with a 1-palmitoyl-2-oleoyl-*sn*-glycero-3-phosphocholine (POPC) bilayer doped with 10 mol% of 1,2-dioleoyl-*sn*-glycero-3-phosphoethanolamine-N-[4-(*p*-maleimidomethyl)-cyclohexanecarboxamide] (MCC-DOPE) while the silica substrates are coated with gel-phase 1,2-dipalmitoyl-*sn*-glycero-3-phosphocholine (DPPC) doped with 10 mol% 1,2-dipalmitoyl-*sn*-glycero-3-phosphoethanolamine-*N*-[4-(*p*-maleimidomethyl)cyclohexanecarboxamide] (MCC-DPPE). The silicate sphere is coated with a POPC bilayer doped with 10 mol% of MCC-DOPE while the silica substrates are coated with DPPC doped with 10 mol% MCC-DPPE. Maleimide functionalized lipids (10 mol%) were chosen to mimic the high density of sugars displayed by g-200 proteoglycans. DPPC was used to provide stability in the contact zone and to minimize detachment of the bilayer from the surface. Formation of SSMs was achieved by vesicle spreading and monitored by fluorescence microscopy. Fluid bilayers display diffusion coefficients of 1.4 ± 0.1 $\mu m^2/s$ as determined by fluorescence recovery after photobleaching—only slightly reduced compared to giant liposomes or free-standing bilayers.[15] Coupling of the epitopes was quantified by reflectometric interference spectroscopy (RIfS), revealing a coupling efficiency of 50% for **2**. Details of the experimental procedures can be found in the SI.

Figure 1 shows a compilation of typical force retraction curves obtained from colloidal probe microscopy. Membrane-coated silicate spheres were brought in contact for a dwell time of 1 s and subsequently retracted from the surface (Figure 1a–c). Interaction forces in the absence of disaccharides attached to the SSMs exhibit a rupture force of 25–50 pN that is entirely abolished in the presence of EDTA-containing buffer (Figure 1a). We attribute the background force to calcium-mediated interaction between the choline headgroups. Attachment of disaccharide **1** lacking the sulfato group to the lipid bilayers did only lead to a small shift in interaction force compared to that in the absence of sugar epitopes (Figure 1d).

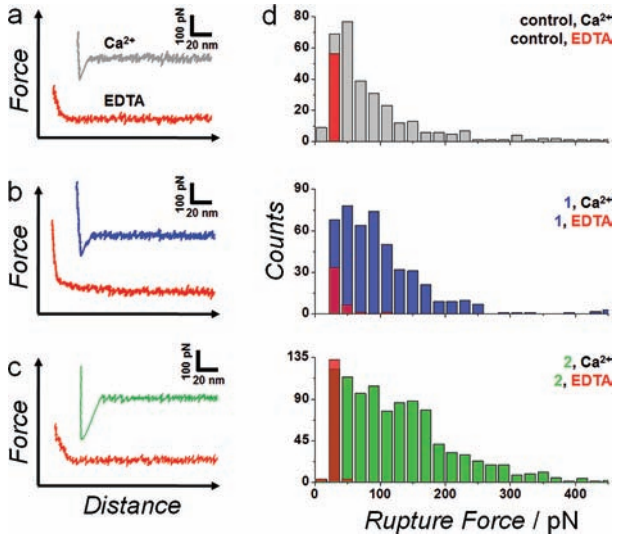

Figure 1. Typical force retraction curves of membrane-coated colloidal probes with different functionalizations (a–c) and corresponding rupture force histograms (d). (a) No disaccharide epitopes, (b) disaccharide **1**, and (c) disaccharide **2** attached to maleimide-bearing phospholipids (10 mol %) in a DPPC (substrate) and POPC (probe) matrix. Interactions were probed in calcium buffer before (gray) and after functionalization of membranes with disaccharide **1** (blue) and **2** (green), respectively. Force curves obtained in EDTA containing buffer are shown in red. Measurements were performed at a loading rate of 10 nN/s, 1 s dwell time, and a load force of 200 pN prior to retraction of the cantilever.

In contrast, coupling of sulfated disaccharides **2** to maleimide groups of the outer membrane leaflets resulted in a shift to larger force that was entirely dependent on the presence of Ca^{2+}. In the presence of **2**, membrane tethers were frequently formed. Addition of Ca^{2+} chelators such as EDTA (5 mM after rinsing with buffer) abolished any attractive interaction in all cases (red semitransparent histograms). The histogram of forces found for the homomeric interaction between **2** in the presence of 10 mM Ca^{2+} displays several resolvable peaks that we attribute to attractive background interaction between the bilayers at low forces and the disruption of nanoclusters of various sizes at higher forces. These data establish the necessity of the sulfato group for self-recognition, and the essential role of Ca^{2+} ions in mediating the interactions. Along these lines, Vliegenthart and co-workers found that the interaction between carbohydrates derived from *M. prolifera* is completely abolished upon substitution with other divalent cations such as Mg^{2+} or Mn^{2+}, while Cd^{2+} preserves the interaction.[8,11]

Figure 2 shows rupture force histograms recorded at different loading rates illustrating that the contact zone between membrane-coated colloidal probe and the SSM comprises a number of parallel bonds. The estimation of the exact number of participating bonds requires some general thermodynamic and kinetic considerations.

The formation of nanoclusters composed of more than a single dimeric bond is driven by an intricate competition between enthalpic and entropic contributions on the one hand and kinetic assembly schemes on the other hand.[13,17–19] Smith and Seifert argued that cluster size is governed by binding enthalpy favoring growing clusters and dispersion driven by gain in entropy.[19,20] In essence, weak bonds with a free energy of only few k_BT do not lead to large clusters. Those bonds are only formed by stochastic matching upon contact between substrate and probe,

dx.doi.org/10.1021/ja210304j | J. Am. Chem. Soc. 2012, 134, 3326–3329

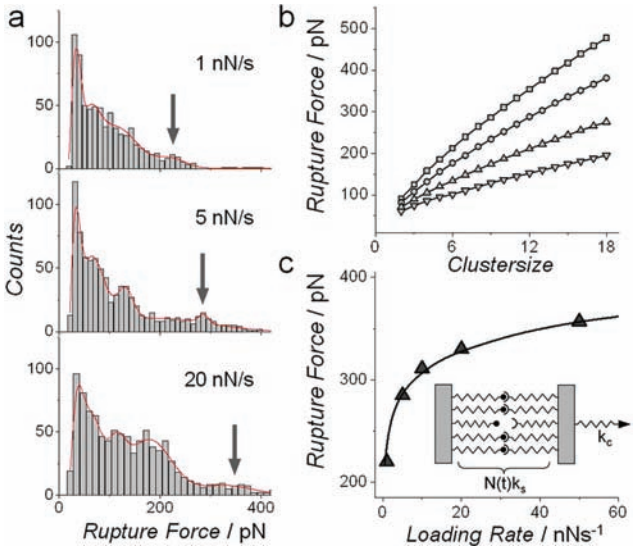

Figure 2. (a) Rupture force histograms for different loading rates subject to multipeak fitting of five Gaussian functions to capture the various cluster sizes. (b) Rupture force as a function of cluster size obtained by solving the ordinary differential equation of time dependent dissolution of multiple bonds subject to a linear force ramp as a function of bond stiffness: k_s = 0.1 (□), 0.025 (○), 0.01 (△), and 0.005 N m^{-1} (▽). Parameters for modeling: k_{off} = 0.14 s^{-1}, x_u = 0.36 nm, μ = 1 nN/s. (c) Rupture force of clusters consisting of N_b = 5 bonds as a function of loading rate (▲) subject to fitting the parameters of eq 1 represented by the solid line. Assumed parameters: k_{on} = 0, k_{off} = 0.0015 s^{-1}, k_c = 0.01 N/m, k_s = 3.4 mN/m, x_u = 0.25 nm.

while in contrast strong bonds accumulate in the contact zone. Assuming that we deal with weak bonds and only one mobile membrane, accumulation of bonds in the contact zone can be largely excluded.

Rupture of multiple bonds under dynamic loading can be described by a simple kinetic model introduced by Bell and further investigated by Seifert.[21−23] The rate equation for the time-dependent decrease in the number of bonds $N(t)$ from initially N_b reads

$$\partial_t N = -N(t)k_{off}\exp(F(t)x_u/k_BT) + (N_b - N(t))k_{on} \quad (1)$$

with the dissociation rate k_{off}, the association rate k_{on} in equilibrium, and the force per bond $F(t) = k_{sys}vt = \mu t$, with v, the pulling velocity and μ, the loading rate.[23] The spring constant, $k_{sys} = k_c k_s/(N(t)k_s + k_c)$, depends on the spring constant of the cantilever k_c and that produced by the involved molecules $N(t)k_s$, with k_s the stiffness of a single-bonded molecule. The rupture force of this deterministic model is defined by $F_{rup} = \mu\tau$, with τ the lifetime of the cluster defined by $N(\tau) = 1$. Equation 1 is solved numerically with initial condition $N(t{=}0) = N_b$ (see SI for details). The strategy to obtain as many intrinsic parameters of the system from force spectroscopy works as follows. First, the number of bonds involved in the colloidal probe measurement is estimated from measuring the mean stiffness of the clusters and its variance. Alternatively, counting the number of maxima occurring in a rupture force histogram also serves this purpose (*vide infra*). The former method also provides the molecular stiffness k_s of a single-bonded molecule. The second step comprises rupture force measurements as a function of loading rate to determine the equilibrium off-rate k_{off} at zero load and the distance between barrier and bound state distance, x_u. Therefore, these two parameters contained in eq 1 are fitted to the mean rupture force of a given cluster size as a function of loading rate (Figure 2).

Figure 2a shows the impact of loading rate on the rupture force. As expected, the rupture forces shift to larger values with higher pulling velocity. Importantly, the deterministic model predicts that rupture forces do not linearly increase with cluster size as expected from a simple superposition of parallel springs carrying a shared load. In fact, softer molecular springs with lower k_s-values produce less dynamic strength (F_{rup}) for a given cluster size (Figure 2b). This behavior can be rationalized by considering two limiting cases in current force experiments in which the distance and not the force is controlled. Seifert distinguishes shared load in which $k_s \gg k_c$ and the force per bond depends on the $N(t)$ existing bonds from the noncooperative case where $N_b k_s \ll k_c$ and the force per bond is independent of $N(t)$.[23,24] It is therefore mandatory to estimate the molecular stiffness prior to a detailed analysis of the dynamic strength. We computed $\langle N_b k_s\rangle$ from >400 force curves and by assuming a Poisson distribution of k_s used the identity $k_s = \sigma^2/\langle N_b k_s\rangle$ to determine k_s = 3.4 mN/m and $N_b \approx 4$. According to the rupture force histograms that were best described by five Gaussians (Figure 2a), we assigned cluster sizes comprising three to five sugar−sugar bonds. This is in good accordance to estimates from Poisson statistics of k_s. A third way to guess the initial cluster size very coarsely is to divide the measured rupture force of the cluster by the rupture force of a single bond. De Souza et al. measured an average rupture force of 30 ± 6 pN for the individual bond between two sulfated disaccharides in the presence of calcium, which corresponds to approximately seven to eight bonds participating in the cluster.[11] In the following analysis we assume N_b = 5 as derived from the rupture force histograms. Figure 2c shows a fit of eq 1 to the dynamic strength of the largest clusters comprising five parallel bonds identified from the force histograms (figure 2a, arrows).

The experimental data could be best described by an equilibrium off-rate of $k_{off} \approx 0.0015$ s^{-1}, and a potential width of x_u = 0.25 nm that are in good accordance with force spectroscopy data obtained from Anselmetti and co-workers measuring the dynamic strength of a single g-200−g-200 interaction.[5] The potential width is slightly closer to the barrier than predicted (x_u = 0.35 nm). The loss in strength due to a closer distance to the barrier might be rationalized by the more complex oligosaccharides involved in the homomeric g-200 interaction rendering the deviation within a reasonable range.

Considering the rather large membrane-coated probe used in our study with a radius of 7.5 μm, the dynamic strength of only very few bonds are assessed after a dwell time of 1s. We attribute this to a combination of various contributions. The effective contact area is very small considering that only those bonds carry the load efficiently that reside at the bottom of the potential which is in the center of the adhesion zone. This effect is enhanced by the finite surface roughness of the probe (~0.7 nm rms).[25] Due to the inherent curvature of the probe, bonds are only formed at a distance of 70 nm from the center of the sphere. Taking into account that k_{off} increases exponentially with distance from the center of the spherical probe only few bonds effectively participate in a cluster. Enrichment of bonds in the contact zone is largely prohibited by entropy costs due to the low binding energy of the homodimers. Besides, the nonbound sugar moieties act as repeller molecules that produce repulsion upon close contact. Due to the finite softness of the

dx.doi.org/10.1021/ja210304j | J. Am. Chem. Soc. 2012, 134, 3326−3329

bound molecules, the rupture force becomes less strongly influenced by the number of bonds constituting the cluster, which eventually leads to a systematic underestimation of N_b. In the limiting case of a very soft linker it is conceivable that rupture forces of clusters are independent of the number of participating bonds.

In conclusion, we investigated the formation and dynamic strength defined as the rupture force of carbohydrate nanoclusters between two opposing membranes equipped with disaccharide epitopes derived from the marine sponge *M. prolifera*. The weak binding affinity prevents clustering beyond statistical matching and therefore allows observing the bond breakage from individual bonds to very small ensembles comprising only few dimers. The setup based on colloidal force probe allows monitoring the rupture force as a function of bilayer fluidity, loading rate, and ionic strength in the absence of thermal undulations and minimal non-specific interaction forces. The technique permits measuring the cooperativity of molecular recognition in a chemically and physically defined way.

Compared to single-molecule mechanics, small clusters allow the measurement of the effect of rebinding that enhances the measured strength at low loading rates. The system described here will permit the measurement of kinetics of dimer formation *and* dissolution, with both partners displayed on lipid bilayers. Many biological systems are constructed in this manner and studies of vesicle docking as an initial step in fusion and cellular adhesion will benefit from this general scheme if the epitopes are synthetically accessible.

■ ASSOCIATED CONTENT

Supporting Information

Detailed experimental procedures and analytical data for disaccharides **1** and **2** as well as their precursors, ^{1}H and ^{13}C NMR spectra, RIfS data, and numerical computation of eq 1. This material is available free of charge via the Internet at http://pubs.acs.org.

■ AUTHOR INFORMATION

Corresponding Author

ajansho@gwdg.de

Notes

The authors declare no competing financial interest.

■ ACKNOWLEDGMENTS

D.B.W. thanks the Deutsche Forschungsgemeinschaft (Emmy Noether Fellowship as well as project A5 in SFB 803 "Functionality controlled by organization in and between membranes") and the Fonds der Chemischen Industrie. B.L. gratefully acknowledges financial support from the IMPRS "Physics of Biological and Complex Systems". This work was partially funded by the National Institutes of Health (GM065500 and CA125033 to K.K.).

■ REFERENCES

(1) Bucior, I.; Burger, M. M. *Curr. Opin. Struct. Biol.* **2004**, *14*, 631.
(2) Misevic, G. N.; Finne, J.; Burger, M. M. *J. Biol. Chem.* **1987**, *262*, 5870.
(3) Bucior, I.; Scheuring, S.; Engel, A.; Burger, M. M. *J. Cell Biol.* **2004**, *165*, 529.
(4) Garcia-Manyes, S.; Bucior, I.; Ros, R.; Anselmetti, D.; Sanz, F.; Burger, M. M.; Fernandez-Busquets, X. *J. Biol. Chem.* **2006**, *281*, 5992.
(5) Fernandez-Busquets, X.; Koernig, A.; Bucior, I.; Burger, M. M.; Anselmetti, D. *Mol. Biol. Evol.* **2009**, *26*, 2551.
(6) Spillmann, D.; Thomasoates, J. E.; Vankuik, J. A.; Vliegenthart, J. F. G.; Misevic, G.; Burger, M. M.; Finne, J. *J. Biol. Chem.* **1995**, *270*, 5089.
(7) Santos, J. I.; de Souza, A. C.; Canada, F. J.; Martin-Santamaria, S.; Kamerling, J. P.; Jimenez-Barbero, J. *ChemBioChem* **2009**, *10*, 511.
(8) Haseley, S. R.; Vermeer, H. J.; Kamerling, J. P.; Vliegenthart, J. F. G. *Proc. Natl. Acad. Sci. U.S.A.* **2001**, *98*, 9419.
(9) de Souza, A. C.; Halkes, K. M.; Meeldijk, J. D.; Verkleij, A. J.; Vliegenthart, J. F. G.; Kamerling, J. P. *Eur. J. Org. Chem.* **2004**, 4323.
(10) de Souza, A. C.; Halkes, K. M.; Meeldijk, J. D.; Verkleij, A. J.; Vliegenthart, J. F. G.; Kamerling, J. P. *ChemBioChem* **2005**, *6*, 828.
(11) de Souza, A. C.; Ganchev, D. N.; Snel, M. M. E.; van der Eerden, J. P. J. M.; Vliegenthart, J. F. G.; Kamerling, J. P. *Glycoconjugate J.* **2009**, *26*, 457.
(12) Boulbitch, A.; Guttenberg, Z.; Sackmann, E. *Biophys. J.* **2001**, *81*, 2743.
(13) Weikl, T. R.; Asfaw, M.; Krobath, H.; Rozycki, B.; Lipowsky, R. *Soft Matter* **2009**, *5*, 3213.
(14) Abdulreda, M. H.; Moy, V. T. *Biophys. J.* **2007**, *92*, 4369.
(15) Lorenz, B.; Keller, R.; Sunnick, E.; Geil, B.; Janshoff, A. *Biophys. Chem.* **2010**, *150*, 54.
(16) Schuy, S.; Treutlein, B.; Pietuch, A.; Janshoff, A. *Small* **2008**, *4*, 970.
(17) Smith, A.-S.; Sackmann, E. *ChemPhysChem* **2009**, *10*, 66.
(18) Fenz, S. F.; Smith, A.-S.; Merkel, R.; Sengupta, K. *Soft Matter* **2011**, *7*, 952.
(19) Smith, A.-S.; Seifert, U. *Soft Matter* **2007**, *3*, 275.
(20) Fenz, S. F.; Bihr, T.; Merkel, R.; Seifert, U.; Sengupta, K.; Smith, A.-S. *Adv. Mater.* **2011**, *23*, 2622.
(21) Bell, G. I. *Science* **1978**, *200*, 618.
(22) Bell, G. I.; Dembo, M.; Bongrand, P. *Biophys. J.* **1984**, *45*, 1051.
(23) Seifert, U. *Phys. Rev. Lett.* **2000**, *84*, 2750.
(24) Erdmann, T. Ph.D. thesis, University of Potsdam, 2005.
(25) van Zwol, P. J.; Palasantzas, G.; van de Schootbrugge, M.; de Hosson, J. T. M.; Craig, V. S. J. *Langmuir* **2008**, *24*, 7528.